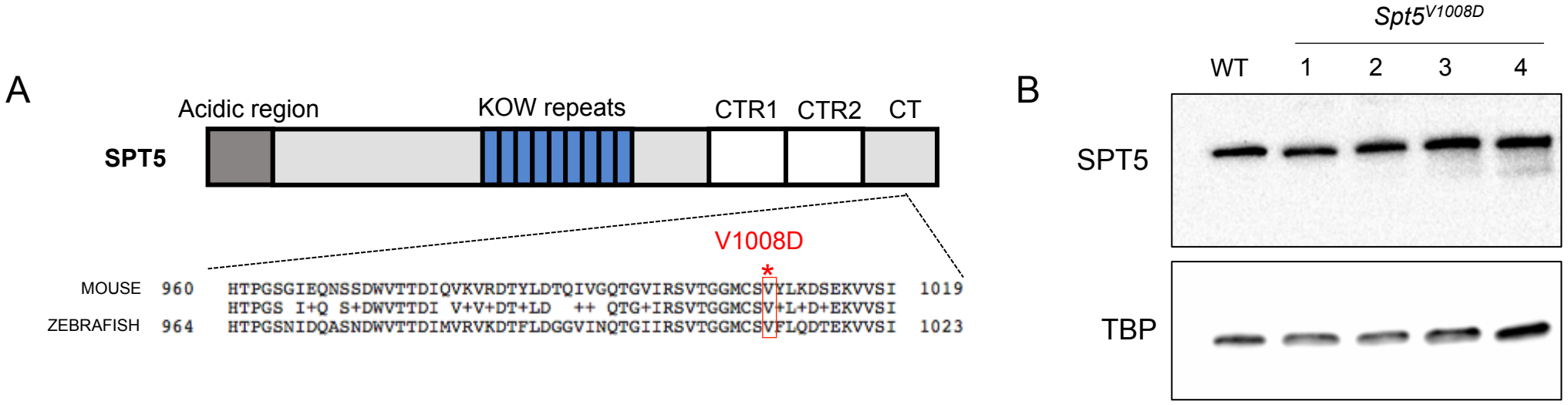

Figure S1. Generation of *Spt5* mutant ESCs. Related to Figure 1

A. Schematic of SPT5 protein and zoomed alignment of C-terminus containing the region of the V1008D mutation in mouse (V1012D in zebrafish).

B. Western blots comparing the levels of SPT5 between wild type and mutant ESCs. TBP serves as a loading control.

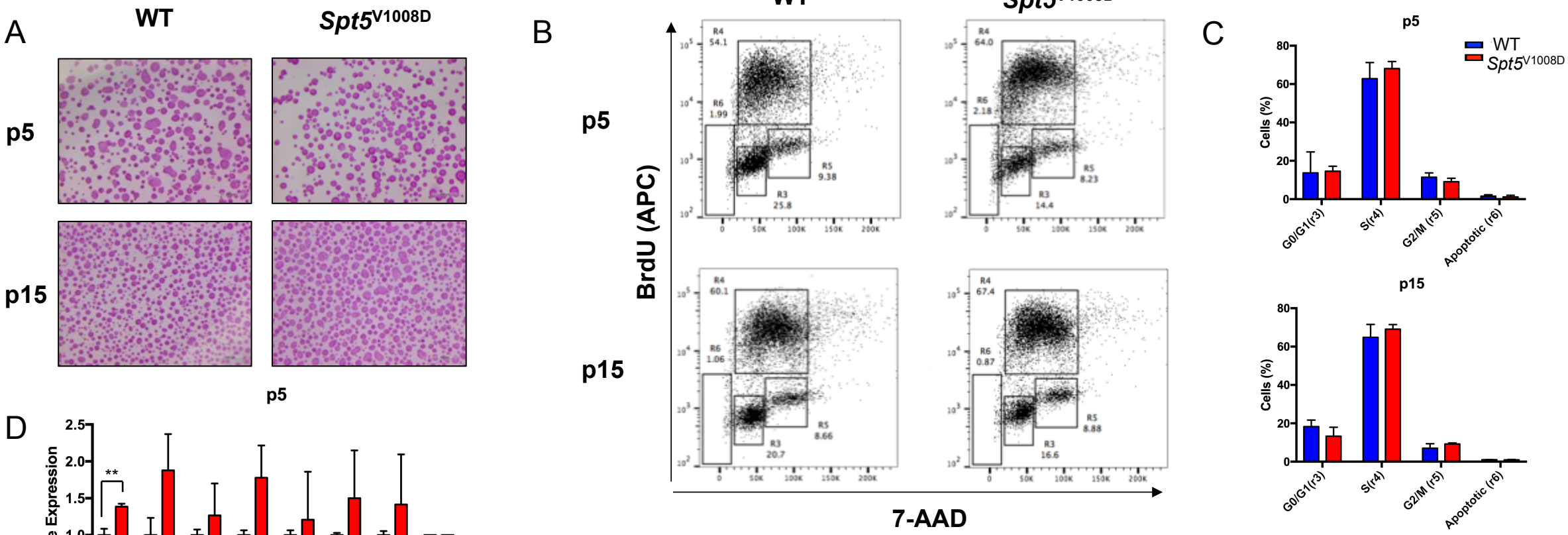

Figure S2.Affect of long term culturing on wild-type and Spt5^{V1008D} ESCs. Related to Figure 1

A. Representative images of alkaline phosphatase staining of wild-type and *Spt5^{V1008D}* homozygous ESCs at 5th(p5) and 15th(p15) passages in culture.

B. Representative flow-cytometry plots for BrdU and 7-AAD at early (p5) and late (p15) passages

C. Quantification of cell cycle profiles (in B) at early (p5) and late (p15) passages

D. Quantitative RT-PCR comparing mRNA levels of ESC markers in wild-type and *Spt5^{V1008D}* ESCs at early (p5) and late passages (p15). Gene expression is normalized to *Gapdh* and presented as fold change relative to wild-type levels (n=3, mean ± SEM).

A

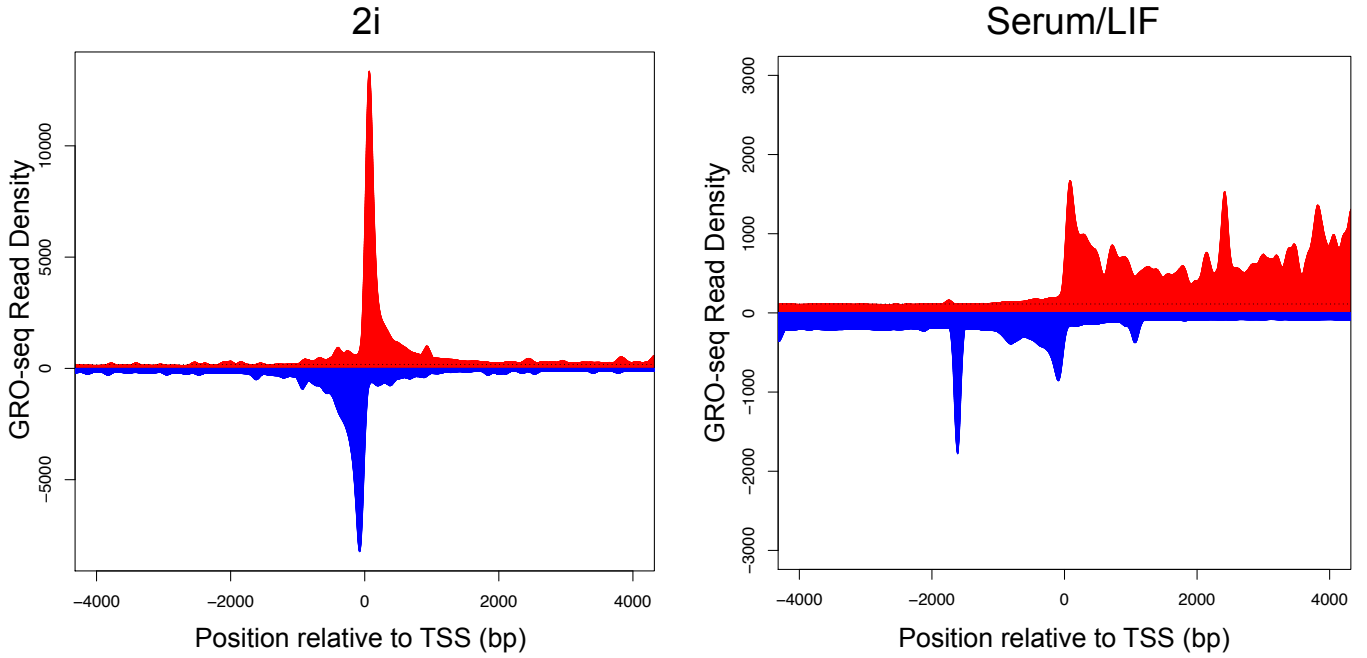

B

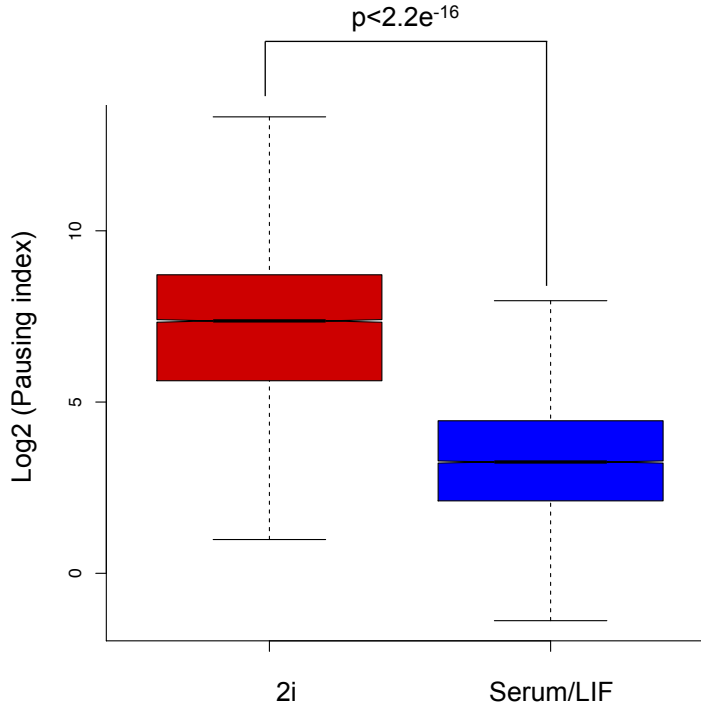

C

Serum/LIF	2i
Transcription, DNA-templated	Transcription, DNA-templated
Regulation of transcription, DNA-templated	Regulation of transcription, DNA-templated
Transport	Transport
Cell cycle	Cellular response to DNA damage stimulus
Cellular response to DNA damage stimulus	Cell cycle

Figure S3. ESC culturing conditions affect transcriptionally paused Pol II levels. Related to Figure 2

A. Metagene analysis showing transcriptionally engaged Pol II occupancy centered at the transcription start site (TSS) measured by GRO-seq on sense and anti-sense strands in serum-free 2i (left) and serum/LIF media (right) in wild type ESCs.

B. Boxplot analysis comparing PI between 2i (red) and *serum/LIF* (blue) culturing conditions.

C. Top 5 Gene Ontology Categories for highly paused genes in cells culturing in serum- vs. 2i-containing medium (PI>2, p<0.001)

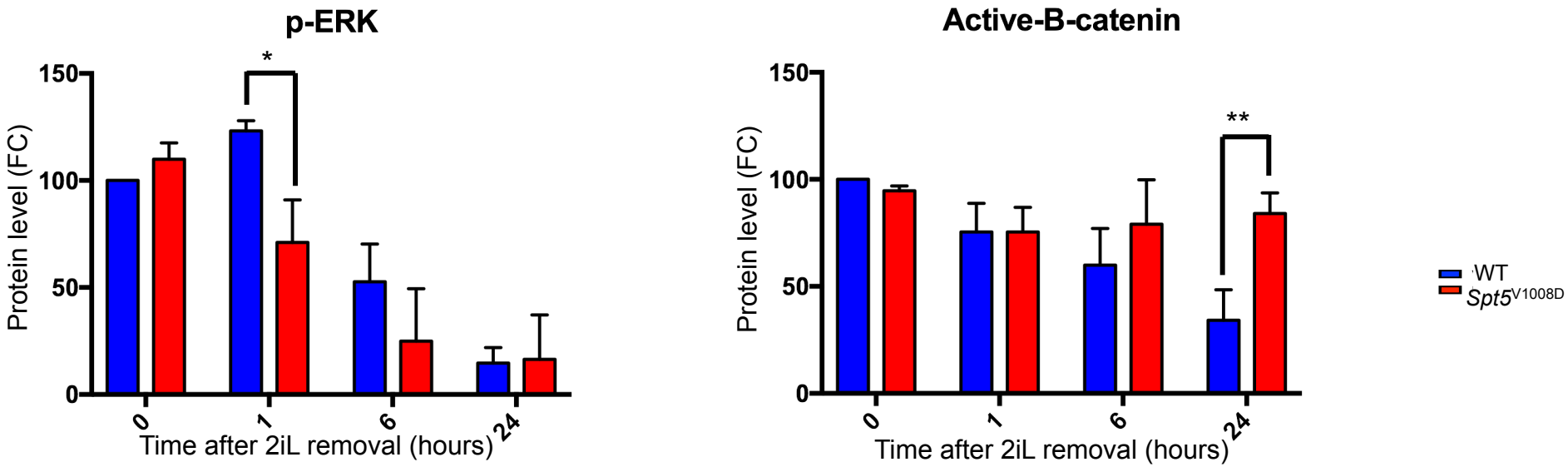

Figure S4 Quantification of western blot in Fig. 4A by imageLAB. Protein level is normalized to B-ACTIN and presented as fold change relative to control samples at time 0 hours. (n=3; mean+-SEM; *P<.05; **P < .01).

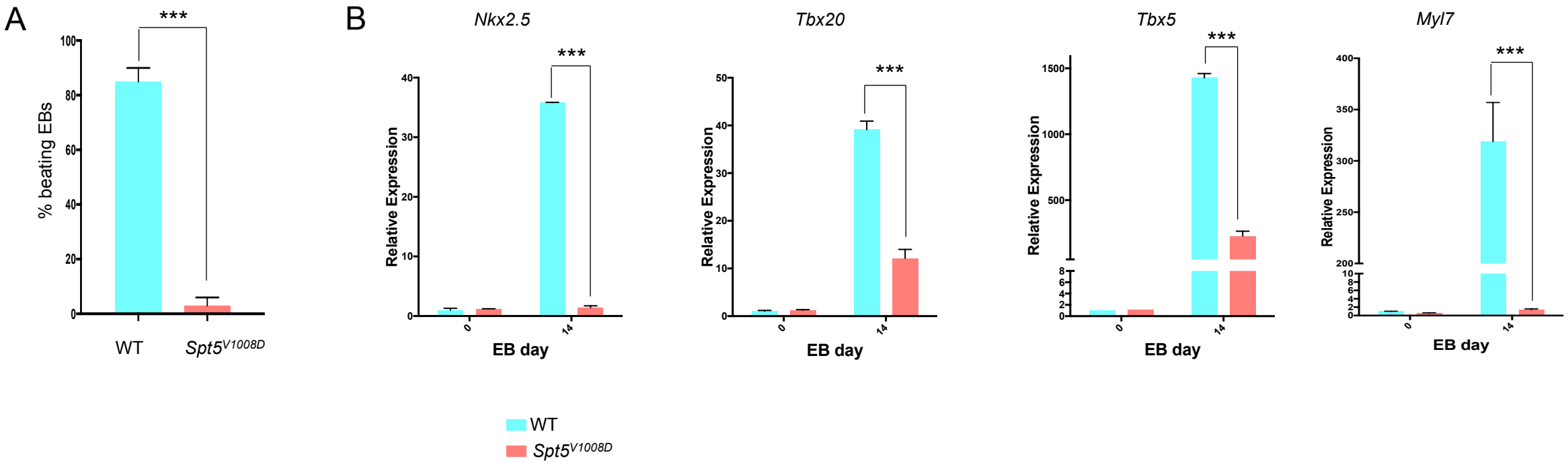

Figure S5. *Spt5* mutant ESCs show defects in cardiac differentiation. Related to Figure 4.

A. Frequencies of beating embryoid bodies (EB) at day-12 of differentiation. Results are represented as mean ± SEM from 3 independent experiments. 50-60 EBs were counted in each experiment. $p<0.001$.

B. Quantitative RT-PCR comparing mRNA levels of cardiac markers in wild type and *Spt5* mutant ESCs at day-0 and day-14 of differentiation. Gene expression is normalized to *Gapdh* and presented as fold change relative to wild type (n=3, mean ± SEM, $p<0.001$).

Table S1. Top ontology terms (p<0.001) for genes that show reduced pausing index (>1.5-fold) in *Spt5*^{V1008D} mutant ESCs, Related to figure 2.

Term	P-Value
GO:0006351~transcription, DNA-templated	1.15E-14
GO:0000122~negative regulation of transcription from RNA polymerase II promoter	1.17E-14
GO:0006355~regulation of transcription, DNA-templated	2.52E-14
GO:0045944~positive regulation of transcription from RNA polymerase II promoter	2.55E-10
GO:0045893~positive regulation of transcription, DNA-templated	1.52E-08
GO:0016310~phosphorylation	2.86E-08
GO:0090090~negative regulation of canonical Wnt signaling pathway	7.12E-07
GO:0043065~positive regulation of apoptotic process	1.47E-06
GO:0032922~circadian regulation of gene expression	3.00E-06
GO:0008285~negative regulation of cell proliferation	3.13E-06
GO:0007275~multicellular organism development	3.63E-06
GO:0006468~protein phosphorylation	4.48E-06
GO:0008284~positive regulation of cell proliferation	5.81E-06
GO:0006915~apoptotic process	9.81E-06
GO:0045892~negative regulation of transcription, DNA-templated	1.48E-05
GO:0016569~covalent chromatin modification	1.72E-05
GO:0006470~protein dephosphorylation	1.96E-05
GO:0030154~cell differentiation	2.13E-05
GO:0001666~response to hypoxia	4.87E-05
GO:0030155~regulation of cell adhesion	6.00E-05
GO:0008584~male gonad development	6.50E-05
GO:0042493~response to drug	7.61E-05
GO:0043406~positive regulation of MAP kinase activity	1.12E-04
GO:0008283~cell proliferation	1.35E-04
GO:0021762~substantia nigra development	1.72E-04
GO:0008152~metabolic process	2.02E-04
GO:0006469~negative regulation of protein kinase activity	2.75E-04
GO:0006357~regulation of transcription from RNA polymerase II promoter	2.86E-04
GO:0051726~regulation of cell cycle	3.37E-04
GO:0030308~negative regulation of cell growth	3.85E-04
GO:0006366~transcription from RNA polymerase II promoter	4.23E-04
GO:0043524~negative regulation of neuron apoptotic process	4.87E-04
GO:0010718~positive regulation of epithelial to mesenchymal transition	4.96E-04
GO:0016055~Wnt signaling pathway	5.54E-04
GO:0007179~transforming growth factor beta receptor signaling pathway	6.05E-04
GO:0051384~response to glucocorticoid	6.05E-04
GO:0042127~regulation of cell proliferation	6.08E-04
GO:0071456~cellular response to hypoxia	6.22E-04
GO:0008652~cellular amino acid biosynthetic process	7.17E-04
GO:0007623~circadian rhythm	7.38E-04
GO:0014070~response to organic cyclic compound	7.72E-04
GO:0045597~positive regulation of cell differentiation	8.21E-04
GO:0016311~dephosphorylation	8.86E-04
GO:0016575~histone deacetylation	9.73E-04

Table S2. Top ontology terms (p<0.001) for genes that show downregulation (≥1.5fold) in *Spt5*^{V1008D} mutant ESCs, Related to figure 3

GO:0006811~ion transport	1.19E-12
GO:0007275~multicellular organism development	2.10E-11
GO:0030154~cell differentiation	3.91E-09
GO:0019233~sensory perception of pain	2.24E-07
GO:0034765~regulation of ion transmembrane transport	5.81E-07
GO:0007507~heart development	7.27E-07
GO:0007399~nervous system development	4.03E-06
GO:0006816~calcium ion transport	4.86E-06
GO:0055085~transmembrane transport	5.48E-06
GO:0071300~cellular response to retinoic acid	9.17E-06
GO:0045893~positive regulation of transcription, DNA-templated	1.08E-05
GO:0042472~inner ear morphogenesis	2.51E-05
GO:0042475~odontogenesis of dentin-containing tooth	4.16E-05
GO:0007219~Notch signaling pathway	7.49E-05
GO:0042391~regulation of membrane potential	9.25E-05
GO:0007155~cell adhesion	9.43E-05
GO:0008285~negative regulation of cell proliferation	9.94E-05
GO:0007169~transmembrane receptor protein tyrosine kinase signaling pathway	1.25E-04
GO:0007605~sensory perception of sound	2.17E-04
GO:0001569~patterning of blood vessels	3.20E-04
GO:0006813~potassium ion transport	3.30E-04
GO:0018101~protein citrullination	3.53E-04
GO:0001503~ossification	3.55E-04
GO:0001570~vasculogenesis	4.14E-04
GO:0048565~digestive tract development	4.37E-04
GO:0006351~transcription, DNA-templated	4.78E-04
GO:0006810~transport	6.05E-04
GO:0021516~dorsal spinal cord development	6.88E-04
GO:0045766~positive regulation of angiogenesis	7.36E-04
GO:0035019~somatic stem cell population maintenance	7.73E-04
GO:0007165~signal transduction	7.76E-04
GO:0000122~negative regulation of transcription from RNA polymerase II promoter	8.24E-04
GO:0034220~ion transmembrane transport	8.82E-04
GO:0045944~positive regulation of transcription from RNA polymerase II promoter	9.26E-04
GO:0006811~ion transport	1.19E-12

Table S3. Table S2. Top ontology terms ($p<0.001$) for genes that show upregulation (≥1.5fold) in *Spt5*^{V1008D} mutant ESCs, Related to figure 3

GO:0009952~anterior/posterior pattern specification	2.14E-09
GO:0007275~multicellular organism development	1.71E-06
GO:0000122~negative regulation of transcription from RNA polymerase II promoter	1.04E-05
GO:0006351~transcription, DNA-templated	2.86E-05
GO:0045944~positive regulation of transcription from RNA polymerase II promoter	3.38E-05
GO:0048706~embryonic skeletal system development	5.74E-05
GO:0006355~regulation of transcription, DNA-templated	9.12E-05
GO:0048704~embryonic skeletal system morphogenesis	2.04E-04
GO:0030154~cell differentiation	2.20E-04
GO:0009887~organ morphogenesis	3.02E-04
GO:0030326~embryonic limb morphogenesis	4.32E-04
GO:0009954~proximal/distal pattern formation	6.52E-04
GO:0008284~positive regulation of cell proliferation	8.64E-04
GO:0009952~anterior/posterior pattern specification	2.14E-09

Supplemental Experimental Procedures

Generation of *Spt5V1008D* mESCs

The targeting vector for the mutant allele consisted of 773bp fragment located 5' of *Supt5h* exon 28, a loxP site-flanked hygromycin selection cassette followed by a 373 bp 3' homology arm (chromosomal location) located on exon 30 of the endogenous *Supt5h* locus. The V1008D mutation was introduced to the left homology arm using QuickChange Site Directed Mutagenesis Kit (Agilent). We designed an sgRNA block (IDT) that targeted Intron 29 of the endogenous loci. The Crispr/Cas9 plasmid, vector carrying the sgRNA block and the donor vector were introduced to wild-type ESCs using Neon Transfection system (Thermo Fisher). ESC clones that have integrated the donor DNA were selected using 150 ng/ml hygromycin B (Corning).

Upon two rounds of electroporation homozygous *Supt5h* knock-in (V1008D) clones were generated. Integration to the endogenous *Supt5h* loci were screened by PCR using primers outside the homology arms followed by *Sanger* sequencing. Confirmed homozygous clones were treated with a Cre-expressing adenovirus (VectorBiolabs) for removal of the hygromycin cassette and successful removal was confirmed using PCR and sequencing.

Alkaline Phosphatase Staining

Alkaline phosphatase staining was performed using the alkaline phosphatase detection kit (Stemgent) according to the manufacturer's instructions. Shortly, ESCs were fixed for 5 minutes at room temperature with the fixation solution. Fixation was followed by two washes of 1X PBS plus 0.05% Tween-so. Staining solution was added to the cells and plates were incubated at room temperature in dark for 15 minutes. Staining reaction was stopped by two washes in PBS.

BrdU Cell Proliferation Assay

BrdU labeling and flow cytometric analysis of cell cycle was performed using the BD Pharmingen^{TM} BrdU Flow Kit (552598) according to the manufacturer's instructions. Briefly, Cells were labelled in 10 uM BrdU in 2i media, followed by collection and fixation. Cells were then permeabilized and treated with DNAse (300ug/mL in DPBS) for 1 hr at 37°C. Afterwards, cells were stained with anti-BrdU antibody followed by total DNA staining by 7-AAD and acquired by a flow cytometer at a low flow rate.

Western Blotting

ESCs were collected using 0.25% trypsin-EDTA, quenched in ESC media and washed with PBS (Gibco). Samples were placed into 1.5 ml tubes and lyzed in RIPA buffer (Sigma) containing Protease inhibitor cocktail (Roche) on ice for 30 minutes. Protein concentration was determined using Bradford assay (BioRad) and equal amounts of protein were loaded**.** Antibodies were: p44/42 MAPK (Erk1/2) (Cell Signaling, 9102), Phospho-p44/42 MAPK (Erk1/2) (Cell Signaling, 9101), Active-B-Catenin (Millipore, clone 8E7, 05-665), SPT5 (Santa Cruz, H-300, sc-28678), TFIID (TBP) (Santa Cruz, sc-204), Beta-Actin (Santa Cruz, sc-47778).

Global Run-on sequencing

GRO-seq experiments were performed as described in (Core et al., 2008) in wild type and mutant mESCs grown in 2i media or serum containing ESC media. Nuclei were collected by swelling attached cells for 10 minutes in cold lysis buffer (10 mM Tris-HCl pH 8, 10 mM NaCl, 3 mM $CaCl_2$, 2 mM $MgCl_2$, 0.5 % NP40, 0.5 mM DTT, 300 mM sucrose, 3 U/ml Superase-IN RNAse inhibitor (Ambion), 1 tablet Roche protease inhibitor/ 50 ml), then lyzed by vigorous pipetting in cold lysis buffer, centrifuged and washed again with lysis buffer. Nuclei were resuspended in freezing buffer as in (Core et al., 2008) as $5x10^6$ nuclei per 100 ul and stored at -80°C until use.

As described in Williams et al., 2015, final concentration of CTP (Roche) was increased 10fold in the run-on reaction than that used in (Core et al., 2008) to 10uM to avoid a misrepresentation of C-rich regions in the data set. The run-on reaction was terminated after 5 minutes by direct addition of Trizol-LS (Invitrogen).

After base-hydrolysis and end repair, samples were immunoprecipitated twice with BrdU beads and poly-adenyl tailed, and then reverse-transcribed. The cDNA was PAGE purified and amplified with 11 cycles of PCR (Illumina). Libraries were PAGE purified for products larger than 140 bp.

Embryoid Body formation

ESCs were titrated to a single cell suspension using trypsin-EDTA and resuspended in differentiation medium (mESC medium with 15% FBS without LIF). Hanging drops were prepared at 300-500 cells/ 30 ul drop in differentiation medium. After three days of differentiation in hanging drops, embryoid bodies were transferred to

low-attachment dishes and cultured in a shaking (50 rpm) incubator. Embryoid bodies were collected at indicated time points for further analysis**.**

Analysis of GRO-seq Data

The GRO-seq data were analyzed using software described before (Hah et al., 2011; Luo et al., 2014) and the approaches described below. Scripts and other related information about the analyses can be obtained by contacting the corresponding author (X.B.).

***Quality Control and Read Alignment*.**

Quality control for the Gro-seq data was performed using the FastQC tool (http://www.bioinformatics.babraham.ac.uk/projects/fastqc/). Gro-seq reads were aligned to the mouse reference genome (mm10), using the BWA aligner (Li and Durbin, 2010). Only uniquely mapping reads were considered for the downstream analyses. After combining the replicates, uniquely mappable reads for each strand were converted into bigWig files using the writeWiggle function in the groHMM tool for visualization in UCSC genome browser (Quinlan and Hall, 2010).

***Gene Ontology Analyses*.**

Gene Ontology Analyses were performed using the DAVID (Database for Annotation, Visualization, and Integrated Discovery) tool (Dennis et al., 2003).

Differential Expression Analyses.

The differential expression analyses were performed using the Bioconductor package called edgeR (Robinson et al., 2010). A window of +300bp to +13kb from the transcription start site (TSS) was used for the analysis. This window was chosen in order to exclude the reads from RNA polymerase that are engaged at the promoter region and to allow enough time for the elongation of newly initiated Pol II. Also, this ensured that only the gene body activity level estimates were taken into account to measure only the productively elongating RNA polymerase. In order to capture significant changes in gene body activity between the two conditions (WT and mutant), only the significantly ($p<0.0001$) regulated genes with at least 1.5 fold change were considered for further analyses.

Metagene Analyses.

Metagene analyses were performed to show the distribution of average GRO-seq read densities ±4 kb surrounding the transcription start site (TSS) using the metagene functions in the GRO-seq package. Metagene analyses were also performed for the up regulated and down regulated genes to show the difference in the read density distributions in the two conditions.

Analysis of ATAC-seq Data

Quality control for the ATAC-seq data was performed using the FastQC tool (http://www.bioinformatics.babraham.ac.uk/projects/fastqc/). ATAC-seq reads were aligned to the mouse reference genome (mm10), using the BWA aligner (Li and Durbin, 2010). Only uniquely mapping reads were considered for the downstream analyses. After combining the replicates, uniquely mappable reads were converted into bigWig files using BEDTools for visualization in UCSC genome browser (Quinlan and Hall, 2010).

Data Integration

We compared out GRO-seq differential expression data and ATAC-seq data with previously published ChIP-seq data from (Joshi et al., 2015; Marks et al., 2012). These published ChIP-seq data consist of E14-2i wildtype cells for enrichment in different histone modifications and polycomb proteins. We measured the signal or read density of this data, and the signal density of our ATAC-seq data under differentially regulated up and down genes from our GRO-seq data. This was done to check which set of these genes display changes in regulation in histone modifications and polycomb proteins.

References

Core, L.J., Waterfall, J.J., and Lis, J.T. (2008). Nascent RNA sequencing reveals widespread pausing and divergent initiation at human promoters. Science *322*, 1845-1848.
Dennis, G., Jr., Sherman, B.T., Hosack, D.A., Yang, J., Gao, W., Lane, H.C., and Lempicki, R.A. (2003). DAVID: Database for Annotation, Visualization, and Integrated Discovery. Genome biology *4*, P3.
Hah, N., Danko, C.G., Core, L., Waterfall, J.J., Siepel, A., Lis, J.T., and Kraus, W.L. (2011). A rapid, extensive, and transient transcriptional response to estrogen signaling in breast cancer cells. Cell *145*, 622-634.
Joshi, O., Wang, S.Y., Kuznetsova, T., Atlasi, Y., Peng, T., Fabre, P.J., Habibi, E., Shaik, J., Saeed, S., Handoko, L.*, et al.* (2015). Dynamic Reorganization of Extremely Long-Range Promoter-Promoter Interactions between Two States of Pluripotency. Cell stem cell *17*, 748-757.
Li, H., and Durbin, R. (2010). Fast and accurate long-read alignment with Burrows-Wheeler transform. Bioinformatics *26*, 589-595.
Luo, X., Chae, M., Krishnakumar, R., Danko, C.G., and Kraus, W.L. (2014). Dynamic reorganization of the AC16 cardiomyocyte transcriptome in response to TNFalpha signaling revealed by integrated genomic analyses. BMC genomics *15*, 155.
Marks, H., Kalkan, T., Menafra, R., Denissov, S., Jones, K., Hofemeister, H., Nichols, J., Kranz, A., Stewart, A.F., Smith, A.*, et al.* (2012). The transcriptional and epigenomic foundations of ground state pluripotency. Cell *149*, 590-604.
Quinlan, A.R., and Hall, I.M. (2010). BEDTools: a flexible suite of utilities for comparing genomic features. Bioinformatics *26*, 841-842.
Robinson, M.D., McCarthy, D.J., and Smyth, G.K. (2010). edgeR: a Bioconductor package for differential expression analysis of digital gene expression data. Bioinformatics *26*, 139-140.